

Pyridyl-Directed C–H and C–Br Bond Activations Promoted by Dimer Iridium-Olefin Complexes

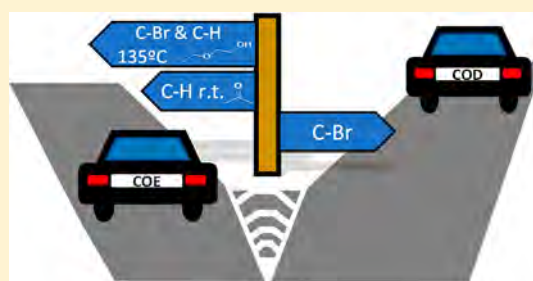
Pierre-Luc T. Boudreault,[‡] Miguel A. Esteruelas,^{*,†,‡} Erik Mora,[†] Enrique Oñate,^{†,‡} and Jui-Yi Tsai[‡]

[†]Departamento de Química Inorgánica, Instituto de Síntesis Química y Catálisis Homogénea (ISQCH), Centro de Innovación en Química Avanzada (ORFEO-CINQA), Universidad de Zaragoza-CSIC, 50009 Zaragoza, Spain

[‡]Universal Display Corporation, 375 Phillips Boulevard, Ewing, New Jersey 08618, United States

Supporting Information

ABSTRACT: Complexes $[\text{Ir}(\mu\text{-Cl})(\eta^2\text{-C}_8\text{H}_{14})_2]_2$ (**1**) and $[\text{Ir}(\mu\text{-Cl})(\eta^4\text{-C}_8\text{H}_{12})_2]_2$ (**2**) promote the pyridyl-directed *ortho*-CH and *ortho*-CBr activations of the phenyl substituent of 2-(2-bromophenyl)pyridine. The formed products depend upon the olefin of the dimer, which governs the kinetic preference of the activation. The cyclooctene complex **1** reacts with the substituted heterocycle to give $(\eta^2\text{-C}_8\text{H}_{14})_2\text{Ir}(\mu\text{-Cl})_2\text{Ir}\{\kappa^2\text{-C,N-}[\text{C}_6\text{BrH}_3\text{-py}]\}_2$ (**3**), in acetone, at room temperature. Treatment of **3** with K(acac) affords $\text{Ir}(\text{acac})(\eta^2\text{-C}_8\text{H}_{14})_2$ (**4**) and $\text{Ir}(\text{acac})\{\kappa^2\text{-C,N-}[\text{C}_6\text{BrH}_3\text{-py}]\}_2$ (**5**; acac = acetylacetonate). Under more severe conditions, 2-ethoxyethanol under reflux, the reaction of **1** with the heterocycle gives a yellow solid, which yields a 5:82:7 mixture of **5**, $\text{Ir}(\text{acac})\{\kappa^2\text{-C,N-}[\text{C}_6\text{BrH}_3\text{-py}]\}\{\kappa^2\text{-C,N-}[\text{C}_6\text{H}_4\text{-py}]\}$ (**6**), and $\text{Ir}(\text{acac})\{\kappa^2\text{-C,N-}[\text{C}_6\text{H}_4\text{-py}]\}_2$ (**7**) by reaction with K(acac). In acetone or toluene, at room temperature, 2-(2-bromophenyl)pyridine breaks the chloride bridges of dimer **2** to form $\text{IrCl}(\eta^4\text{-C}_8\text{H}_{12})\{\kappa^1\text{-N-}[\text{py-C}_6\text{BrH}_4]\}$ (**8**), which evolves into $\text{IrClBr}\{\kappa^2\text{-C,N-}[\text{C}_6\text{H}_4\text{-py}]\}(\eta^4\text{-C}_8\text{H}_{12})$ (**9**) as a result of the oxidative addition of the *ortho*-CBr of the phenyl substituent to the metal center. Treatment of **9** with Ag_2O in acetylacetonate leads to $\text{Ir}(\text{acac})\{\kappa^2\text{-C,N-}[\text{C}_6\text{H}_4\text{-py}]\}\{\kappa^1\text{-C, } \eta^2\text{-}[\text{C}_8\text{H}_{12}\text{-}(\text{C}^3\text{-acac})]\}$ (**10**), as a consequence of the replacement of the halides by an O,O-chelate acac ligand and the outside to metal nucleophilic attack of a second acac group to the diene C–C double bond disposed *trans* to bromide.



INTRODUCTION

Haloarenes are ubiquitous organic substrates in homogeneous transition metal-mediated catalysis.¹ Their chemical properties and reactions are distinct from those of the hydrocarbon counterparts, since the C–X bond (X = F, Cl, Br, I) influences of different manner the diverse C–H bonds of the molecule. As a consequence, the metal-promoted σ -bond activation reactions present a particular challenge because they may occur at several C–H positions. In addition, the C–H bond rupture competes with the C–X bond cleavage.²

The activation of a particular C–H bond in haloarenes is of great relevance because it allows its selective direct functionalization.³ Usually, this activation is kinetically and thermodynamically controlled by steric reasons. As a consequence, the less hindered *meta* and *para* M–C bonds are formed, although the metal center moves toward fluoride substituents which favor the *ortho* disposition.⁴ On the other hand, the oxidative addition of the C–X bond (X = Cl, Br, I) to a low valent transition metal is the key step in organometallic-catalyzed cross-coupling reactions, which are among the industrial technologies of the highest significance,⁵ and in the dehalogenation of these substrates mediated by metals,⁶ which is also a high-priority target from an environmental point of view because their accumulation is a serious health hazard.

Palladium(0) complexes are the most common catalysts for cross-coupling reactions.⁷ According to this, there are a significant number of theoretical and experimental works centered about the oxidative addition of C–X bonds (X = Cl, Br, I) to zerovalent d¹⁰ metal centers.⁸ In the past years, examples have appeared where rhodium catalysts enable coupling of haloarenes,⁹ whereas other ones have proved to be particularly efficient for dehalogenation reactions.¹⁰ In the same vein, rhodium complexes have shown to favor the oxidative addition of C–X bonds with regard to that of C–H bonds from a thermodynamic point of view,¹¹ although both activations appear to be kinetically competitive.¹²

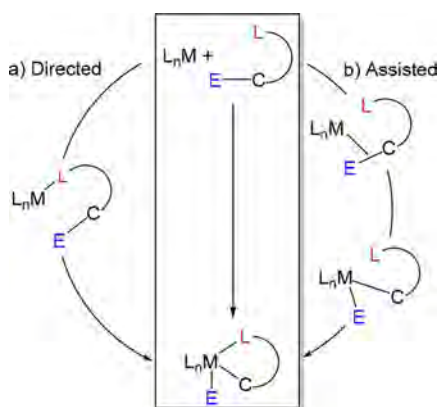
Iridium catalysts are not usual in cross-coupling reactions. Consistently, the competitive C–H versus C–X (X = Cl, Br, I) oxidative additions on iridium have been less studied than with zerovalent d¹⁰ metal centers and with rhodium. Milstein and co-workers have reported the *ortho*-CH oxidative addition of chloro- and bromobenzene to $[\text{Ir}(\text{PNP}^*)]^+$ (PNP* = 2,6-bis((di-*tert*-butylphosphino)methyl)pyridine).¹³ Ozerov and co-workers have described a similar preference for the *ortho*-CH oxidative addition of the same substrates to the neutral species $\text{Ir}(\text{PNP})$ (PNP = bis(2-(diisopropylphosphino)-4-methylphenyl)amino).¹⁴ However, in the latter, the preference

Received: July 17, 2018

is only kinetic since the products from the C–X bond activation (X = Cl, Br) are thermodynamically favored.¹⁵

Understanding the factors that control the preference of the cleavage of C–H versus C–X is crucial to design optimal transition-metal-catalyzed processes. One of the major goals to approach the issue is to eliminate the asymmetry in the C–H bond activation, in this class of substrates, selecting a position equivalent to the C–X bond. In order to perform such selection, we have replaced a hydrogen atom at position *ortho* of bromobenzene by a 2-pyridyl group. Complexes having heterometalatings are usually more stable than their non-chelated analogues. According to this, the introduction of a Lewis base in the organic substrate to stabilize the formed M–C bond is considered to be one of the most efficient ways to promote the selective activation of a particular C–E bond (E = H, X).¹⁶ From a mechanistic point of view, the σ -bond activation reactions carried out under these conditions can be directed or assisted (Scheme 1).¹⁷ The first of them involve the

Scheme 1. Mechanisms for σ -Bond Activations in the Presence of an Intramolecular Lewis Base



initial coordination of the heteroatom, which kinetically directs the C–E bond activation and stabilizes the resulting M–C bond (a).¹⁸ However, the C–E bond activation is the first step in the second case (b); the subsequent coordination of the heteroatom provides thermodynamic selectivity to the resulting product from a proximal cleavage.¹⁹

Olefin complexes are useful starting compounds in the iridium chemistry.²⁰ In the search for information about the factors that control the competitive ruptures of C–H versus C–X with this element, we have studied the reactions of the known dimers $[\text{Ir}(\mu\text{-Cl})(\eta^2\text{-C}_8\text{H}_{14})_2]_2$ (**1**) and $[\text{Ir}(\mu\text{-Cl})(\eta^4\text{-C}_8\text{H}_{12})_2]_2$ (**2**) with 2-(2-bromophenyl)pyridine. In this paper,

we demonstrate that the olefin of the starting compound directs the cleavage.

RESULTS AND DISCUSSION

C–H Bond Activation. Treatment of the cyclooctene complex **1** with 2.5 mol of 2-(2-bromophenyl)pyridine in acetone, at room temperature, for 24 h leads to a very insoluble yellow solid, which corresponds to the dinuclear species $(\eta^2\text{-C}_8\text{H}_{14})_2\text{Ir}(\mu\text{-Cl})_2\text{Ir}\{\kappa^2\text{-C,N-[C}_6\text{BrH}_3\text{-py)]}_2$ (**3**), according to its C, H, N-elemental analysis. This compound is formed in 80% yield and is a consequence of the selective *ortho*-CH bond activation of the phenyl substituent of the pyridine, the hydrogenation of a quarter of the coordinated olefin, and the release of the other quarter (Scheme 2). Related 1,5-cyclooctadiene derivatives bearing an $\text{Ir}\{\kappa^2\text{-C,N-[C}_6\text{H}_4\text{-py)]}_2$ fragment have been previously reported by Severin and co-workers.²¹ The presence of the $\text{Ir}\{\kappa^2\text{-C,N-[C}_6\text{BrH}_3\text{-py)]}_2$ moiety in **3** is strongly supported by the MALDI-TOF spectrum of the obtained solid in dimethyl sulfoxide, which shows the corresponding peak with an *m/z* of 659.0. In agreement with the existence of both iridium fragments $\text{Ir}(\eta^2\text{-C}_8\text{H}_{14})_2$ and $\text{Ir}\{\kappa^2\text{-C,N-[C}_6\text{BrH}_3\text{-py)]}_2$ in **3**, the addition of the latter to a methanol solution of potassium acetylacetonate (K(acac)) quantitatively yields after 72 h, at room temperature, an equimolar mixture of the previously reported iridium(I) compound $\text{Ir}(\text{acac})(\eta^2\text{-C}_8\text{H}_{14})_2$ ²² (**4**) and the new iridium(III) derivative $\text{Ir}(\text{acac})\{\kappa^2\text{-C,N-[C}_6\text{BrH}_3\text{-py)]}_2$ (**5**).

Complex **5** was isolated as a yellow solid and characterized by X-ray diffraction analysis. Figure 1 shows a view of the molecule. The geometry around the metal center can be rationalized as a distorted octahedron with the pyridyl groups occupying *trans* positions ($\text{N–Ir–N} = 176.0(4)^\circ$). In the perpendicular plane, the oxygen atoms of the acetylacetonate ligand lie *trans* to the metalated carbon atoms of the phenyl groups ($\text{O–Ir–C} = 173.7(3)^\circ$). In accordance with the high symmetry of the molecule, the methyl groups of the acac ligand display a singlet at 1.79 ppm in the ¹H NMR spectrum.

Activations C–H and C–Br. The insolubility of **3** and the mild conditions used for its formation suggest that the *ortho*-CH bond activation of the phenyl substituent of the pyridine is kinetically favored with regard to the *ortho*-CBr bond activation, in agreement with the previously mentioned results of Milstein and Ozerov. In order to investigate the thermodynamic preference and the influence of the solvent, we carried out the reaction between **1** and the pyridine, in 2-ethoxyethanol, and at both 135 °C and room temperature, a similar experimental procedure to those employed to prepare the iridium(III) dimers $[\text{Ir}(\mu\text{-Cl})\{\kappa^2\text{-C,N-[C}_6\text{R}_4\text{-py)]}_2]_2$.²³ Under these conditions, the stirring of **1** with 4.1 mol (135 °C) or 6.0 mol (r.t.) of 2-(2-bromophenyl)pyridine for 12 h

Scheme 2. *ortho*-CH Bond Activation of 2-(2-Bromophenyl)pyridine Promoted by **1**

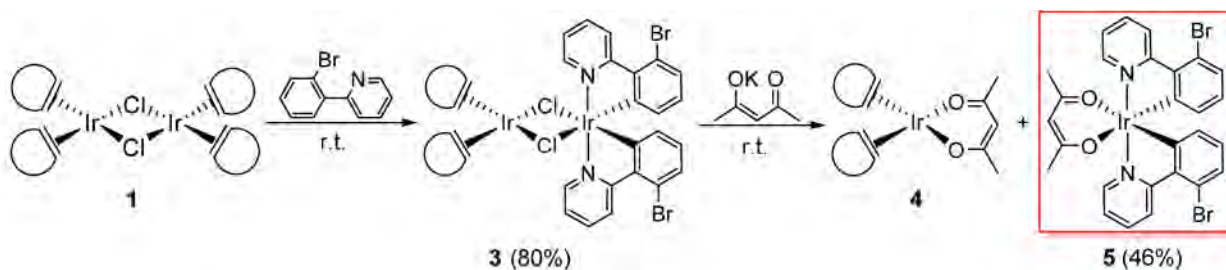




Figure 1. ORTEP diagram of complex **5** (50% probability ellipsoids). Hydrogen atoms are omitted for clarity. Selected bond lengths (Å) and angles (deg): Ir–C = 1.988(9), Ir–N = 2.023(7), Ir–O = 2.153(6), N–Ir–N = 176.0(4), O–Ir–C = 173.7(3).

also affords a very insoluble yellow solid. However, in this case, its MALDI-TOF spectrum in dimethyl sulfoxide reveals the presence of three different fragments $\text{Ir}\{\kappa^2\text{-C,N-[C}_6\text{BrH}_3\text{-py]}\}_2$ ($m/z = 658.9$), $\text{Ir}\{\kappa^2\text{-C,N-[C}_6\text{BrH}_3\text{-py]}\}\{\kappa^2\text{-C,N-[C}_6\text{H}_4\text{-py]}\}$ ($m/z = 578.9$), and $\text{Ir}\{\kappa^2\text{-C,N-[C}_6\text{H}_4\text{-py]}\}_2$ ($m/z = 501.0$). As expected, treatment of the yellow solid with K(acac) in tetrahydrofuran, for 1.5 h, at 60 °C quantitatively yields a mixture of **5**, the tris-heteroleptic complex $\text{Ir}(\text{acac})\{\kappa^2\text{-C,N-[C}_6\text{BrH}_3\text{-py]}\}\{\kappa^2\text{-C,N-[C}_6\text{H}_4\text{-py]}\}$ (**6**) and the previously described compound $\text{Ir}(\text{acac})\{\kappa^2\text{-C,N-[C}_6\text{H}_4\text{-py]}\}_2$ (**7**) in a 5:82:13 molar ratio according to the ^1H NMR spectrum of the reaction crude. The composition of the mixture indicates that the *ortho*-CH and *ortho*-CBr ruptures are competitive, from a thermodynamic point of view, and are equally favored (Scheme 3).

The major product, complex **6**, was separated from the mixture by column chromatography, as a yellow solid in 42% yield with regard to **1**, and was characterized by X-ray diffraction analysis. The structure (Figure 2) proves the tris-heteroleptic nature of the molecule. The geometry around the iridium atom resembles that of **5** with N(1)–Ir–N(2), O(1)–Ir–C(22), and O(2)–Ir–C(11) angles of 174.3(7)°, 172.3(7)°, and 173.6(9)°, respectively. In agreement with the presence of two different metalated phenyl groups disposed *trans* to the acac ligand, the latter displays two methyl resonances at 1.82 and 1.79 ppm in the ^1H NMR spectrum and two methyl signals at 28.7 and 28.8 ppm and two carbonyl resonances at 185.2 and 185.4 ppm in the $^{13}\text{C}\{^1\text{H}\}$ NMR spectrum.

C–Br Bond Activation. The addition of 2.1 mol of 2-(2-bromophenyl)pyridine to acetone solutions of the 1,5-cyclooctadiene derivative **2** at room temperature produces the instantaneous precipitation of a yellow solid, which changes its color into white after 2 h. When the reaction is carried out in toluene, the same white solid is obtained. However, the intermediate yellow solid is soluble. The ^1H and $^{13}\text{C}\{^1\text{H}\}$ NMR spectra of its toluene- d_8 solutions at 223 K reveal that the pyridine initially breaks the chloride bridges of the dimer to form the square-planar iridium(I) complex $\text{IrCl}(\eta^4\text{-C}_8\text{H}_{12})\{\kappa^1\text{-N-[py-C}_6\text{BrH}_4]\}$ (**8**), which displays four olefinic CH resonances at 4.83, 4.69, 3.13, and 2.64 ppm in the

Scheme 3. Activations *ortho*-CH and *ortho*-CBr of 2-(2-bromophenyl)pyridine Promoted by **1**, Including $\text{IrX}\{\kappa^2\text{-C,N-[C}_6\text{R}_4\text{-py]}\}_2$ Fragments of Dimers $[\text{Ir}(\mu\text{-X})\{\kappa^2\text{-C,N-[C}_6\text{R}_4\text{-py]}\}_2]_2$

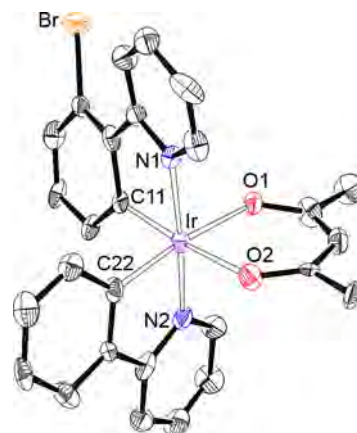
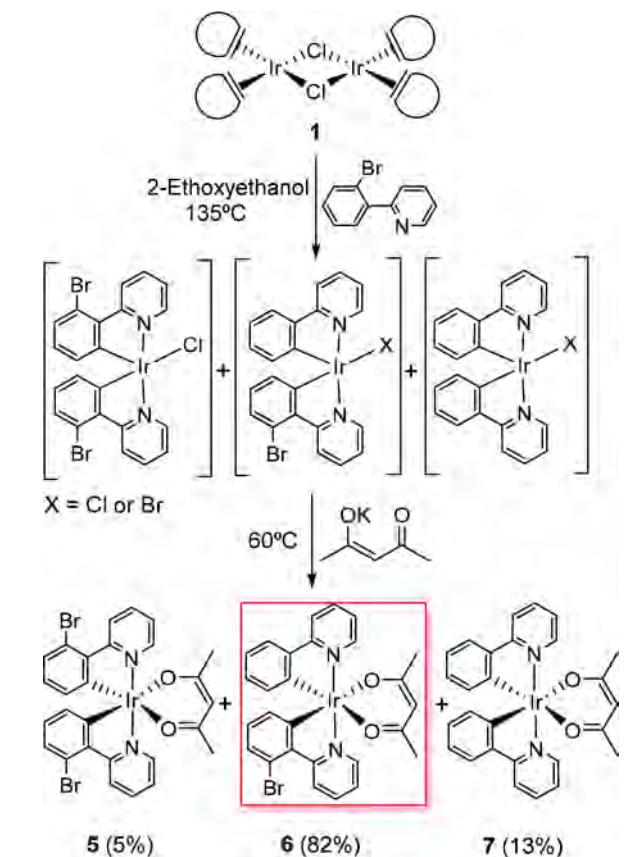
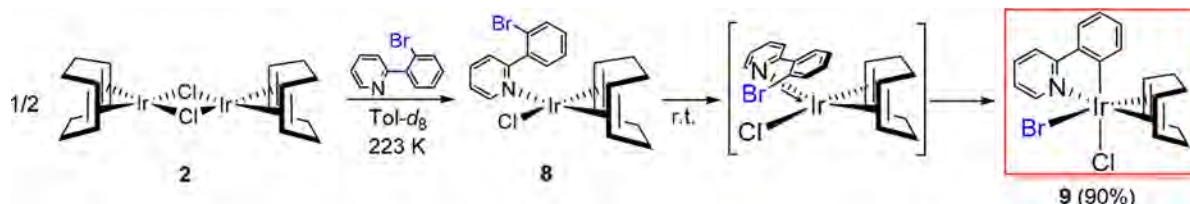


Figure 2. ORTEP diagram of complex **6** (50% probability ellipsoids). Hydrogen atoms are omitted for clarity. Selected bond lengths (Å) and angles (deg): Ir–C(11) = 1.977(19), Ir–C(22) = 2.002(18), Ir–N(1) = 2.07(2), Ir–N(2) = 2.01(2), Ir–O(1) = 2.161(14), Ir–O(2) = 2.142(14), N(1)–Ir–N(2) = 174.3(7), O(1)–Ir–C(22) = 172.3(7), O(2)–Ir–C(11) = 173.6(9).

^1H NMR spectrum and four olefinic C(sp²) signals at 69.0, 67.4, 59.6, and 54.3 ppm in the $^{13}\text{C}\{^1\text{H}\}$ NMR spectrum, in addition to the resonances due to the pyridine and the CH₂ groups of the diolefin. The white solid was isolated in almost quantitative yield and characterized by X-ray diffraction analysis as the iridium(III) derivative $\text{IrClBr}\{\kappa^2\text{-C,N-[C}_6\text{H}_4\text{-}$

Scheme 4. Pyridyl Directed *ortho*-CBr Activation of 2-(2-Bromophenyl)pyridine Promoted by 2

py}}(\eta^4-C_8H_{12}) (9), resulting from the pyridyl-directed *ortho*-CBr bond activation of the phenyl group (Scheme 4).

The structure of 9 (Figure 3) reveals that the C–Br bond activation is a concerted oxidative addition, which takes place

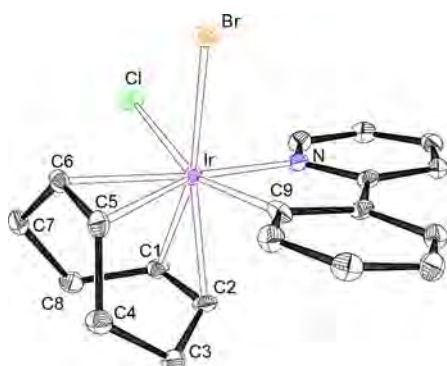


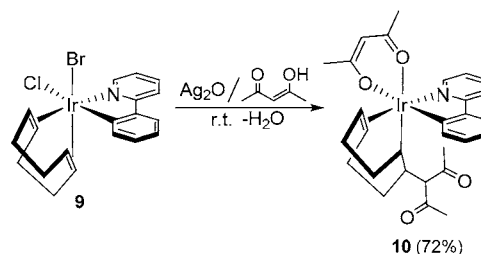
Figure 3. ORTEP diagram of complex 9 (50% probability ellipsoids). Hydrogen atoms are omitted for clarity. Selected bond lengths (Å) and angles (deg): Ir–Br = 2.5274(3), Ir–Cl = 2.4907(8), Ir–N = 2.096(2), Ir–C(9) = 2.075(3), Ir–C(1) = 2.190(4), Ir–C(2) = 2.190(3), Ir–C(5) = 2.218(3), Ir–C(6) = 2.225(3), C(1)–C(2) = 1.398(4), C(5)–C(6) = 1.388(4), Br–Ir–M(1) = 175.21(9), N–Ir–M(2) = 174.8(1), Cl–Ir–C(9) = 159.80(8).

along the olefin–Ir–Cl axis of 8 with the bromine on the chloride ligand.²⁴ Thus, the coordination polyhedron around the iridium atom can be rationalized as a distorted octahedron with the bromide anion disposed *trans* to the C(1)–C(2) olefinic bond (Br–Ir–M(1) = 175.21(9)°; M(1) = midpoint between C(1) and C(2)), whereas the chloride ligand lies *trans* to the metalated phenyl substituent (Cl–Ir–C(9)) = 159.80(8)°, and the pyridyl group is situated *trans* to the olefinic C(5)–C(6) bond (N–Ir–M(2) = 174.8(1)°; M(2) = midpoint between C(5) and C(6)). The 1,5-cyclooctadiene ligand takes its customary “tub” conformation.

The coordinated bonds have lengths of 1.398(4) (C(1)–C(2)) Å and 1.388(4) (C(5)–C(6)) Å, which are longer than the C–C double bonds in the free diolefin (1.34 Å)²⁵ as expected for the usual Chatt–Dewar–Ducanson model. The difference between them is consistent with the different *trans* influences of bromide and pyridine. In agreement with the structure, the ¹H NMR spectrum, in dichloromethane-*d*₂, at room temperature shows four resonances at 5.69, 5.24, 4.52, and 3.21 ppm for the C(sp²)-H hydrogen atoms of the diene. Consistently, the ¹³C{¹H} NMR spectrum displays four signals at 101.2, 91.8, 89.4, and 87.9 ppm for the diene C(sp²) atoms.

Like the C–H bond activation products, complex 9 reacts with the acac anion. In this case, however, the presence of two halides at the metal coordination sphere determines the reaction procedure and the nature of the resulting product (Scheme 5). Treatment of acetylacetonone solutions of 9 with 2.7 mol of silver oxide, at room temperature, for 12 h produces the

Scheme 5. Reaction of 9 with Acetylacetonate



abstraction of the halides and the nucleophilic attack of two acac anions to the Ir{κ²-C,N-[C₆H₄-py]}(η⁴-C₈H₁₂) moiety. One of them attacks the metal center as O,O-chelate, while the C³-carbon atom of the other one is added to the coordinated C–C bond of 9 situated *trans* to the bromide ligand (C(1)–C(2)). As a result of both attacks, complex Ir(acac){κ²-C,N-[C₆H₄-py]}{κ¹-C, η²-[C₈H₁₂-(C³-acac)]} (10) is formed. This compound was isolated as a pale-yellow solid in 72% yield and characterized by X-ray diffraction analysis.

The structure (Figure 4) proves both attacks. The addition to C(1)–C(2) gives rise to an Ir–C(sp³) bond disposed *trans*

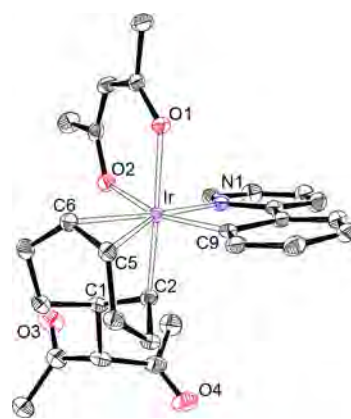
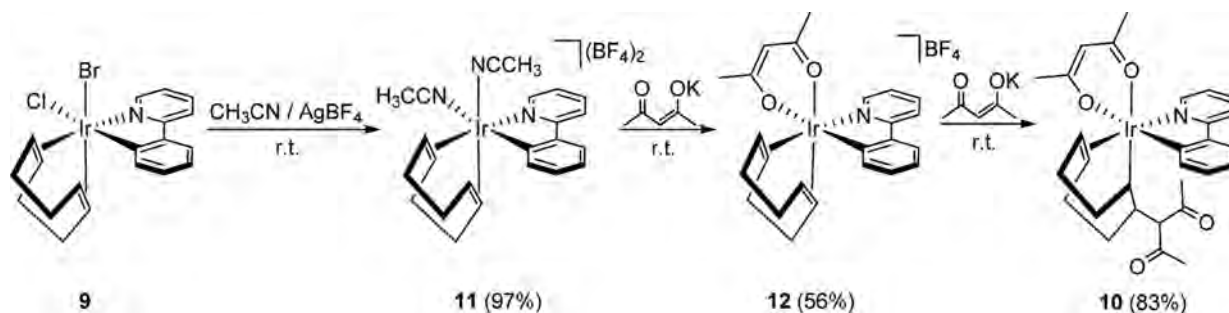


Figure 4. ORTEP diagram of complex 10 (50% probability ellipsoids). Hydrogen atoms are omitted for clarity. Selected bond lengths (Å) and angles (deg): Ir–N(1) = 2.088(2), Ir–O(1) = 2.177(2), Ir–O(2) = 2.143(2), Ir–C(2) = 2.074(2), Ir–C(5) = 2.172(2), Ir–C(6) = 2.169(2), Ir–C(9) = 2.052(2), C(5)–C(6) = 1.391(3), O(1)–Ir–C(2) = 176.51(7), O(2)–Ir–C(9) = 160.62(8), N–Ir–M(2) = 173.33(8).

to an oxygen atom of the O,O-chelate acac group (O(1)–Ir–C(2) = 176.51(7)°), in an octahedral environment. The other oxygen atom of the O,O-chelate acac ligand lies *trans* to the metalated phenyl group (O(2)–Ir–C(9) = 160.62(8)°), whereas the pyridyl ring is situated *trans* to the C(5)–C(6) double bond (N–Ir–M(2) = 173.33(8)°). The functionalized carbocycle coordinates with three different Ir–C bond lengths of 2.074(2) (Ir–C(2)) Å, 2.172(2) (Ir–C(5)) Å, and

Scheme 6. Reaction Sequence Confirming the Outside to Metal Nature of the acac Attack to C(1)–C(2)

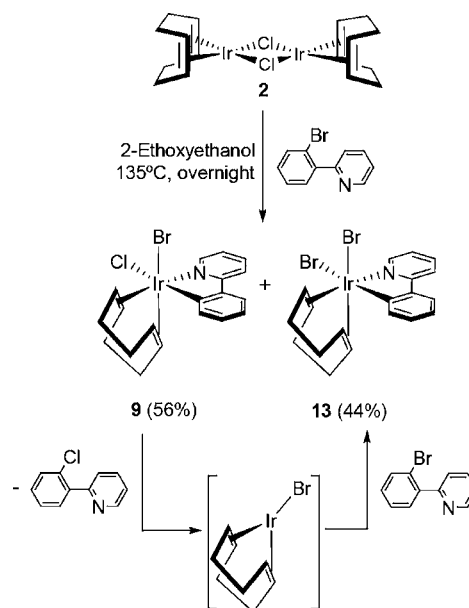


2.169(2) (Ir–C(6)) Å, which agree with those reported for compounds bearing $C_8H_{12}R$ rings similarly linked to iridium(III).²⁶ The length of the coordinated C(5)–C(6) bond of 1.391(3) Å also compares well with the lengths of C(1)–C(2) and C(5)–C(6) in **9**. The iridium atom and the C³-acac group are disposed in a position *anti* with regard to the C_8 ring. This suggests that the addition to C(1)–C(2) takes place outside to the metal. The ¹H and ¹³C{¹H} NMR spectra of **10**, in dichloromethane-*d*₂, at room temperature are consistent with the structure shown in Figure 4 and the spectra of related compounds.^{26,27} In the ¹H NMR spectrum, the most noticeable features are the two olefinic resonances at 5.05 and 4.58 ppm and the signal due to the IrC(sp³)H hydrogen atom, which appears at 1.28 ppm. In the ¹³C{¹H} NMR spectrum, the resonances corresponding to the C(sp²) atoms C(5) and C(6) are observed at 82.8 and 77.4 ppm, whereas the signal due to C(2) appears at 10.5 ppm. The presence of two different acac groups in the molecule is also evident in the IR, which shows a strong ν (CO) band at 1691 cm⁻¹ for the acac group bonded to C(1) and two strong ν (CO) bands at 1584 and 1513 cm⁻¹ for the O,O-chelate ligand.

The outside to metal nature of the attack to C(1)–C(2) was confirmed by the reactions sequence shown in Scheme 6. Complex **9** reacts with AgBF₄ in acetonitrile to give the bis(solvento) compound [Ir{ κ^2 -C,N-[C₆H₄-py]}(η⁴-C₈H₁₂)-(CH₃CN)₂](BF₄)₂ (**11**) which was isolated as a white solid in almost quantitative yield. The addition of 1.0 equiv of K(acac) to methanol solutions of **11** produces the displacement of the coordinated acetonitrile molecules by the O,O-chelate acac ligand. The resulting cationic acac derivative [Ir(acac){ κ^2 -C,N-[C₆H₄-py]}(η⁴-C₈H₁₂)]BF₄ (**12**) was isolated as a yellow solid in 56% yield. The addition of 5.0 equiv of K(acac) to methanol solutions of **12** leads to **10**, as a consequence of the attack of a new acac anion to the C–C double bond disposed *trans* to the acac ligand. The selective addition to one of the two possible C–C double bonds appears to be related to the π -donor ability of the oxygen atom disposed *trans*, which stabilized the π^* orbital of the attacked C–C double bond with regard to the π^* of the C–C double bond situated *trans* to the pyridyl ring.²⁸ Complexes **11** and **12** were characterized by NMR spectroscopy (see the Experimental Section) and X-ray diffraction analysis (see the Supporting Information).

1,5-Cyclooctadiene also favors the C–Br oxidative addition over the C–H bond activation under the same conditions as cyclooctene benefits both activations, C–Br and C–H, in approximately the same extension. Although traces of products resulting from C–H bond activation are also observed, they appear to be less favored than **9**. Treatment of 2-ethoxyethanol solutions of **2** with 4.1 mol of 2-(2-bromophenyl)pyridine, at

135 °C, for 12 h leads to a yellow suspension, from which yellow (<6%) and white solids can be separated. The main component of the first of them is the Ir{ κ^2 -C,N-[C₆BrH₃-py]}{ κ^2 -C,N-[C₆H₄-py]} fragment, resulting from both ruptures C–Br and C–H. The white solid is the soluble component of the reaction crude and is formed by complexes **9** and IrBr₂{ κ^2 -C,N-[C₆H₄-py]}(η⁴-C₈H₁₂) (**13**), which are products from C–Br cleavages. Complex **13** bearing two bromide ligands mutually *cis* disposed is the result of the reductive elimination of 2-(2-chlorophenyl)pyridine from **9** and the subsequent oxidative addition of a new molecule of 2-(2-bromophenyl)pyridine to the generated metal fragment IrBr(η⁴-C₈H₁₂) (Scheme 7). The mutually *cis* disposition of

Scheme 7. Formation of **13**

the bromide ligands is supported by the inequivalence of the CH groups of the coordinated diene. In agreement with this, the ¹H NMR spectrum shows four olefinic CH resonances at 5.80, 5.17, 4.64, and 3.14 ppm and the ¹³C{¹H} NMR spectrum displays four olefinic C(sp²) signals between 35.5 and 28.2 ppm. Complex **13** was prepared as an analytically pure white solid by means of the reaction of [Ir(η⁴-C₈H₁₂)(Me₂CO)_x](BF₄) with 2-(2-bromophenyl)pyridine (see the Experimental Section).

CONCLUDING REMARKS

This study has revealed that dimers $[\text{Ir}(\mu\text{-Cl})(\eta^2\text{-C}_8\text{H}_{14})_2]_2$ and $[\text{Ir}(\mu\text{-Cl})(\eta^4\text{-C}_8\text{H}_{12})]_2$ promote the activations *ortho*-CH and *ortho*-CBr of the phenyl substituent of 2-(2-bromophenyl)pyridine in a competitive manner. The olefin and reaction conditions determine the preferred activation, which is pyridyl directed.

Cyclooctene favors products resulting from the *ortho*-CH bond activation with regard to those generated from C–Br bond rupture, in acetone, at room temperature. Under the same conditions, 1,5-cyclooctadiene however benefits the *ortho*-CBr oxidative addition to the $\text{IrCl}(\eta^4\text{-C}_8\text{H}_{12})$ metal fragment over *ortho*-CH bond activation products. These facts clearly indicate that the kinetic preference of the activation is governed by the olefin of the iridium precursor: while cyclooctene favors *ortho*-CH bond activation products, 1,5-cyclooctadiene benefits the *ortho*-CBr oxidative addition. More severe conditions help the competitive process, but the sense of the preference does not change. Thus, both ruptures *ortho*-CH and *ortho*-CBr occur in the same extension with the cyclooctene dimer, in 2-ethoxyethanol, at 135 °C. Under the same conditions, 1,5-cyclooctadiene continues to favor the *ortho*-CBr oxidative addition, although traces of products resulting from *ortho*-CH bond activation are also observed.

In conclusion, $\text{IrCl}(\text{olefin})$ complexes, which have been one of the cornerstones in the development of the organometallic iridium chemistry, should receive more attention as promoters of σ -bond activation reactions in haloarenes, since they can play a main role in the understanding of the competence between the possible ruptures.

EXPERIMENTAL SECTION

General Information. All reactions were performed under argon using a Schlenk tube or glovebox techniques and dried solvents. Instrumental methods, NMR spectra, and X-ray diffraction analysis information is given in the Supporting Information. The complexes $[\text{Ir}(\mu\text{-Cl})(\eta^2\text{-C}_8\text{H}_{14})_2]_2$ (**1**) and $[\text{Ir}(\mu\text{-Cl})(\eta^4\text{-C}_8\text{H}_{12})]_2$ (**2**) were prepared as published.²⁹ Chemical shifts (expressed in parts per million) are referenced to residual solvent peaks (^1H , $^{13}\text{C}\{^1\text{H}\}$). Coupling constants, *J*, are given in Hz.

Reaction of 1 with 2-(2-Bromophenyl)pyridine in Acetone: Preparation of $(\eta^2\text{-C}_8\text{H}_{14})_2\text{Ir}(\mu\text{-Cl})_2\text{Ir}\{\kappa^2\text{-C,N-[C}_6\text{BrH}_3\text{-py]}\}_2$ (3**).** 2-(2-Bromophenyl)pyridine (293 μL , 1.70 mmol) was added to **1** (600 mg, 0.67 mmol) in 10 mL of acetone. The resulting suspension was stirred for 24 h at room temperature. After this time, a very insoluble pale-yellow solid was formed, which was washed with diethyl ether (3 \times 5 mL) and dried under vacuum. Yield: 611 mg (80%). Anal. Calcd for $\text{C}_{38}\text{H}_{42}\text{Br}_2\text{Cl}_2\text{Ir}_2\text{N}_2$: C, 39.97; H, 3.71; N, 2.45. Found: C, 40.06; H, 3.58, N, 2.99. HR-MS (MALDI-TOF; DMSO): *m/z* calcd for $\text{C}_{22}\text{H}_{14}\text{Br}_2\text{IrN}_2$ [$\text{M} - \text{IrCl}_2(\eta^2\text{-C}_8\text{H}_{14})_2$]⁺: 658.9, found 659.0.

Reaction of 3 with Potassium Acetylacetonate: Preparation of $\text{Ir}(\text{acac})\{\kappa^2\text{-C,N-[C}_6\text{BrH}_3\text{-py]}\}_2$ (5**).** Complex **3** (350 mg, 0.307 mmol) was added to a solution of acetylacetonate (94.5 μL , 0.920 mmol) and KOH (101.3 mg, 1.535 mmol) in 12 mL of methanol. The resulting suspension was stirred for 72 h at room temperature. After this time, the liquid was decanted and the yellow solid was washed with methanol (3 \times 5 mL) and dried under vacuum. Yield: 215 mg (46%). X-ray quality crystals were grown by slow evaporation of a concentrated solution of the solid in dichloromethane at room temperature. Anal. Calcd for $\text{C}_{27}\text{H}_{21}\text{Br}_2\text{IrN}_2\text{O}_2$: C, 42.81; H, 2.79; N, 3.70. Found: C, 42.78; H, 3.07; N, 3.59. HR-MS (electrospray): *m/z* calcd for $\text{C}_{27}\text{H}_{21}\text{Br}_2\text{IrN}_2\text{O}_2$ [M]⁺ 757.9566; found 757.9555. IR (cm^{-1}): ν (C=O) 1582 (m), 1605 (m). ^1H NMR (300 MHz, CD_2Cl_2 , 298 K): δ 9.27 (d, 2H, $^3J_{\text{H-H}} = 8.2$, CH py), 8.53 (d, 2H, $^3J_{\text{H-H}} = 6.4$, CH py), 7.86 (t, 2H, $^3J_{\text{H-H}} = 8.2$, CH py), 7.27 (t, 2H, $^3J_{\text{H-H}} = 6.4$, CH py), 7.13 (d, 2H, $^3J_{\text{H-H}} = 7.7$, CH Ph), 6.47 (t, 2H,

$^3J_{\text{H-H}} = 7.7$, CH Ph), 6.13 (d, 2H, $^3J_{\text{H-H}} = 7.4$, CH Ph), 5.29 (s, 1H, acac-H), 1.79 (s, 6H, CH_3 acac). The low solubility of the solid precluded to obtain its $^{13}\text{C}\{^1\text{H}\}$ NMR spectrum. From the liquors after decantation, $\text{Ir}(\text{acac})(\eta^2\text{-C}_8\text{H}_{14})_2$ (**4**) was separated.²²

Reaction of 1 with 2-(2-Bromophenyl)pyridine in 2-Ethoxyethanol: Preparation of $\text{Ir}(\text{acac})\{\kappa^2\text{-C,N-[C}_6\text{BrH}_3\text{-py]}\}\{\kappa^2\text{-C,N-[C}_6\text{H}_4\text{-py]}\}$ (6**).** 2-(2-Bromophenyl)pyridine (312 μL , 1.83 mmol) was added to **1** (400 mg, 0.446 mmol), in 10 mL of 2-ethoxyethanol. The mixture was stirred overnight at reflux (135 °C), leading a yellow suspension, which was dried under vacuum, and the residue was treated with 3 \times 5 mL of diethyl ether to afford 581 mg of an insoluble yellow powder. HR-MS (MALDI-TOF; DMSO): *m/z* calcd. for $[\text{C}_{22}\text{H}_{14}\text{Br}_2\text{IrN}_2]$ 658.9, found: 658.4. Calcd for $[\text{C}_{22}\text{H}_{15}\text{-BrIrN}_2]$: 579.0, found: 579.1. Calcd for $[\text{C}_{22}\text{H}_{16}\text{IrN}_2]$: 501.0, found: 501.1. Acetylacetonate (67.4 μL , 0.666 mmol) and KOH (44.0 mg, 0.666 mmol) in 2 mL of methanol was added to the yellow powder (439.5 mg, 0.317 mmol) in 15 mL of THF. The mixture was stirred at 60 °C, for 90 min, in a closed system. Then, the solvent was removed under vacuum and the residue was treated with 15 mL of CH_2Cl_2 . The resulting suspension was filtered over Celite to afford a yellow solution, which was concentrated almost to dryness under vacuum. The addition of 5 mL of pentane led to a yellow solid, which was washed with 2 \times 4 mL of pentane and dried under vacuum. The solid was purified by silica column chromatography using toluene-pentane-ethyl acetate (1-3-1) as eluents. Yield: 180.6 mg (42%). X-ray quality crystals were grown by a slow diffusion of pentane in a concentrated solution of the solid in dichloromethane at 4 °C. Anal. Calcd for $\text{C}_{27}\text{H}_{22}\text{BrIrN}_2\text{O}_2$: C, 47.79; H, 3.27; N, 4.13. Found: C, 47.78, H, 3.66, N, 4.16. HR-MS (electrospray): *m/z* calcd. for $\text{C}_{22}\text{H}_{15}\text{BrIrN}_2$ [$\text{M} - \text{acac}$]⁺ 579.0027; found 579.0032. ^1H NMR (300 MHz, CD_2Cl_2 , 298 K): δ 9.26 (m, 1H, CH py), 8.61 (m, 1H, CH py), 8.43 (m, 1H, H py), 7.85 (m, 3H, CH py), 7.60 (dd, 1H, $^3J_{\text{H-H}} = 7.8$; $^4J_{\text{H-H}} = 1.4$, CH Ph), 7.23 (m, 2H, CH py), 7.13 (d, 1H, $^3J_{\text{H-H}} = 7.8$, CH Ph), 6.87 (dt, 1H, $^3J_{\text{H-H}} = 7.5$; $^4J_{\text{H-H}} = 1.3$, CH Ph), 6.70 (dt, 1H, $^3J_{\text{H-H}} = 7.4$; $^4J_{\text{H-H}} = 1.4$, CH Ph), 6.46 (t, 1H, $^3J_{\text{H-H}} = 7.6$, CH Ph), 6.26 (dd, 1H, $^3J_{\text{H-H}} = 7.5$; $^4J_{\text{H-H}} = 1.2$, CH Ph), 6.12 (dd, 1H, $^3J_{\text{H-H}} = 7.5$; $^4J_{\text{H-H}} = 1.3$, CH Ph), 5.29 (s, 1H, CH acac), 1.82 (s, 3H, CH_3 acac), 1.79 (s, 3H, CH_3 acac). $^{13}\text{C}\{^1\text{H}\}$ NMR (75 MHz, CD_2Cl_2 , 298 K): δ 185.4, 185.2 (C=O acac), 168.2, 167.2 (C py), 153.5 (C Ph), 149.0, 148.5 (CH py), 147.3, 145.4, 142.6 (C Ph), 137.8, 137.0 (CH py), 133.4, 132.9, 129.5, 129.3, 128.2, 124.4 (CH Ph), 123.8, 123.1, 122.4 (CH py), 121.5 (CH Ph), 119.5 (C-Br), 119.1 (CH py), 100.8 (CH acac), 28.8, 28.7 (CH_3 acac).

Reaction of 2 with 2-(2-Bromophenyl)pyridine at 223 K: Preparation of $\text{IrCl}(\eta^4\text{-C}_8\text{H}_{12})\{\kappa^1\text{-N-[py-C}_6\text{BrH}_4]\}$ (8**).** An NMR tube was charged with **2** (11.2 mg, 0.0167 mmol) and 0.5 mL of toluene-*d*₈. After the tube was frozen with a cold bath of solid CO_2 and $^i\text{PrOH}$, 2-(2-bromophenyl)pyridine (5.7 μL , 0.033 mmol) was added. After 30 min, the quantitative formation of **8** was observed. ^1H NMR (400 MHz, *tol-d*₈, 223 K): δ 8.93 (d, 1H, $^3J_{\text{H-H}} = 7.7$, CH py), 8.46 (d, 1H, $^3J_{\text{H-H}} = 5.6$, CH py), 7.24 (d, 1H, $^3J_{\text{H-H}} = 8.1$, CH Ph), 7.07 (m, 1H, CH py), 6.71 (m, 2H, CH Ph), 6.53 (t, 1H, $^3J_{\text{H-H}} = 7.7$, CH py), 6.25 (t, 1H, $^3J_{\text{H-H}} = 6.7$, CH Ph), 4.83 (m, 1H, =CH COD), 4.69 (m, 1H, =CH COD), 3.13 (m, 1H, =CH COD), 2.64 (m, 1H, =CH COD), 2.19 (m, 2H, CH_2 COD), 1.63 (m, 2H, CH_2 COD), 1.29 (m, 2H, CH_2 COD), 1.00 (m, 2H, CH_2 COD). $^{13}\text{C}\{^1\text{H}\}$ NMR (100 MHz, *tol-d*₈, 223 K): δ 157.7 (C py), 150.4 (CH py), 139.6 (C Ph), 135.5 (CH py), 132.1 (CH Ph), 130.8 (CH Ph), 129.1 (CH py), 128.7 (CH py), 126.9 (CH Ph), 123.8 (CH Ph), 121.6 (C-Br Ph), 69.0, 67.4, 59.6, 54.3 (=CH COD), 33.4, 31.5, 30.9, 30.4 (CH_2 COD).

Reaction of 2 with 2-(2-Bromophenyl)pyridine in Acetone: Preparation of $\text{IrClBr}\{\kappa^2\text{-C,N-[C}_6\text{H}_4\text{-py]}\}(\eta^4\text{-C}_8\text{H}_{12})$ (9**).** 2-(2-Bromophenyl)pyridine (268.9 μL , 1.56 mmol) was added to **2** (500 mg, 0.744 mmol) in 8 mL of acetone. The mixture was stirred for 2 h to afford a white suspension. The colorless liquor was decanted, and the white solid was washed with 3 \times 5 mL of diethyl ether and dried in vacuo. Yield: 806 mg (90%). X-ray quality crystals were grown by a slow diffusion of diethyl ether in a concentrated solution of the solid in dichloromethane at 4 °C. Anal. Calcd for $\text{C}_{19}\text{H}_{20}\text{BrClIrN}$: C, 40.04;

H, 3.54; N, 2.46. Found: C, 39.70; H, 3.43; N, 2.44. HR-MS (electrospray): m/z calcd for $C_{19}H_{20}BrIrN [M - Cl]^+$ 534.0391; found 534.0387. 1H NMR (300 MHz, CD_2Cl_2 , 298 K): δ 10.10 (ddd, 1H, $^3J_{H-H} = 6.2$; $^4J_{H-H} = 1.5$; $^5J_{H-H} = 0.7$, CH py), 7.98 (m, 3H, Ph), 7.83 (m, 2H, CH Ph + CH py), 7.47 (m, 1H, CH Ph), 7.30 (m, 2H, CH py), 5.69 (t, 1H, $^3J_{H-H} = 7.9$, =CH COD), 5.24 (m, 1H, =CH COD), 4.52 (td, 1H, $^3J_{H-H} = 8.7$, 4.6, =CH COD), 3.51 (m, 1H, CH_2 COD), 3.21 (m, 1H, =CH COD), 2.81–2.61 (m, 2H, CH_2 COD), 2.43 (m, 1H, CH_2 COD), 2.11 (m, 2H, CH_2 COD), 1.68–1.46 (m, 2H, CH_2 COD). $^{13}C\{^1H\}$ NMR (75 MHz, CD_2Cl_2 , 298 K): δ 165.2 (CN py), 149.7 (CH py), 143.1 (C Ph), 142.2 (Ir-C Ph), 139.3 (CH py), 135.3, 132.4, 125.31 (CH Ph), 124.8, 123.0 (CH py), 120.24 (CH Ph), 101.2, 91.8, 89.4, 87.9 (=CH COD), 34.1, 33.3, 29.2, 28.7 (CH_2 COD).

Reaction of 9 with Acetylacetonate: Preparation of $Ir(acac)\{\kappa^2-C,N-[C_6H_4-py]\}\{\kappa^1-C, \eta^2-[C_8H_{12}(C^3-acac)]\}$ (10). Silver oxide (87.1 mg, 0.376 mmol) was added to 9 (200 mg, 0.342 mmol) in 5 mL of acetylacetonate. The mixture was stirred overnight in the absence of light, and the solvent was removed under vacuum. The residue was treated with 15 mL of dichloromethane, and the resulting suspension was filtered over Celite to afford a pale-yellow solution, which was concentrated almost to dryness. The addition of 5 mL of pentane gave rise to the precipitation of a pale-yellow solid which was washed with 3×5 mL of pentane and dried under vacuum. Yield: 160 mg (71.7%). X-ray quality crystals were grown by a slow diffusion of pentane in a concentrated solution of the solid in dichloromethane at 4 °C. Anal. Calcd for $C_{29}H_{34}IrNO_4$: C, 53.36; H, 5.25; N, 2.15. Found: C, 53.33; H, 5.44; N, 2.33. HR-MS (electrospray): m/z calcd for $C_{24}H_{27}IrNO_2 [M - acac]^+$ 554.1666; found 554.1698. IR (cm^{-1}): ν (C=O) 1691 (s), 1584 (s), 1513 (s). 1H NMR (300 MHz, CD_2Cl_2 , 298 K) δ 8.85 (d, 1H, $^3J_{H-H} = 6.02$, CH py), 7.96 (s, 1H, CH py), 7.93 (s, 1H, CH Ph), 7.76 (ddd, 1H, $^3J_{H-H} = 8.4$, 7.3; $^4J_{H-H} = 1.6$, CH py), 7.66 (dd, 1H, $^3J_{H-H} = 7.6$, $^4J_{H-H} = 1.8$, CH Ph), 7.25 (m, 1H, CH py), 7.19 (m, 1H, CH Ph), 7.12 (m, 1H, CH Ph), 5.30 (s, 1H, CH acac), 5.05 (td, 1H, $^3J_{H-H} = 9.1$, 3.0, =CH COD), 4.58 (m, 1H, =CH COD), 3.59 (d, 1H, $^3J_{H-H} = 11.3$, CH acac COD), 2.90 (td, 1H, $^3J_{H-H} = 11.6$, 6.4, CCH COD), 2.24 (s, 3H, CH_3 acac), 2.05 (s, 3H, CH_3 acac COD), 1.63 (s, 3H, CH_3 acac COD), 1.56 (s, 3H, CH_3 acac), 2.45–1.79 (m, 6H, CH_2 COD), 1.68–0.76 (m, 2H, CH_2 COD), 1.28 (d, 1H, $^3J_{H-H} = 6.4$, HC-Ir). $^{13}C\{^1H\}$ NMR (75 MHz, CD_2Cl_2 , 298 K) δ 205.2 (C=O acac COD), 204.8 (C=O acac COD), 187.1 (C=O acac), 183.2 (C=O acac), 165.6 (C py), 145.7 (CH py), 143.7 (C Ph), 143.0 (C-Ir), 137.8 (CH py), 135.6 (CH Ph), 130.4 (CH Ph), 124.5 (CH Ph), 122.6 (CH Ph), 122.0 (CH py), 119.5 (CH py), 101.0 (CH acac), 82.8, 77.4 (=CH COD), 73.4 (CH κ^1 -acac-C), 39.5 (C=O κ^1 -acac-C), 39.4 (CH COD), 30.3 (CH_3 acac COD), 30.1 (CH_3 acac), 29.5 (CH_3 acac COD), 28.5 (CH_2 COD), 28.4 (CH_3 acac), 27.4 (CH_2 COD), 27.1 (CH_2 COD), 10.5 (CH COD).

Reaction of 9 with $AgBF_4$ in Acetonitrile: Preparation of $[Ir\{\kappa^2-C,N-[C_6H_4-py]\}\{\eta^4-C_8H_{12}\}(CH_3CN)_2](BF_4)_2$ (11). Silver tetrafluoroborate (358.6 mg, 1.84 mmol) was added to 9 (500 mg, 0.877 mmol) in 10 mL of acetonitrile. The solution was stirred for 48 h in the absence of light. The resulting suspension was filtered over Celite to afford a colorless solution, which was concentrated almost to dryness. The addition of 5 mL of diethyl ether gave rise to a white solid which was washed with 3×5 mL of diethyl ether and dried under vacuum. Yield 458 mg (97%). X-ray quality crystals were grown by a slow diffusion of diethyl ether in a concentrated solution of the solid in dichloromethane at 4 °C. Anal. Calcd for $C_{23}H_{26}IrN_3(BF_4)_2$: C, 38.89; H, 3.69; N, 5.92. Found: C, 38.78; H, 3.97; N, 6.05. HR-MS (electrospray): m/z calcd for $C_{19}H_{19}IrN [M - (CH_3CN)_2]^+$ 454.1150; found 454.1142. IR (cm^{-1}): ν (BF_4) = 1050, 1021 (s). 1H NMR (300 MHz, CD_2Cl_2 , 298 K): δ 9.27 (d, 1H, $^3J_{H-H} = 6.0$, CH py), 8.09 (m, 2H, CH py), 7.89 (m, 2H, CH Ph), 7.69 (m, 1H, CH py) 7.58 (td, 1H, $^3J_{H-H} = 7.6$, $^4J_{H-H} = 1.9$, CH Ph), 7.51 (m, 1H, CH Ph), 6.50 (t, 1H, $^3J_{H-H} = 7.5$, =CH COD), 5.86 (q, 1H, $^3J_{H-H} = 7.9$, =CH COD), 5.44 (m, 1H, =CH COD), 3.91 (t, 1H, $^3J_{H-H} = 7.4$, =CH COD), 2.99 (s, 3H, CH_3 CH_3CN), 3.23–2.72 (m, 6H, CH_2 COD), 2.41 (s, 3H, CH_3 CH_3CN), 2.36–2.17 (m, 2H, CH_2 COD). $^{13}C\{^1H\}$ NMR (75 MHz, CD_2Cl_2 , 298 K): δ 163.4 (C py), 151.1

(CH py), 142.0 (CH py), 134.8 (CH Ph), 133.9 (CH Ph), 131.6 (C Ph), 127.7 (CH Ph), 126.8 (CH py), 126.6 (CH py), 123.0 (C py), 121.6 (CH Ph), 109.3, 99.7, 98.9, 91.8 (=CH COD), 33.9, 32.0, 28.1, 27.6 (CH_2 COD), 30.1, 30.0 (CH_3CN), 5.2, 4.3 (CH_3CN).

Preparation of $[Ir(acac)\{\kappa^2-C,N-[C_6H_4-py]\}\{\eta^4-C_8H_{12}\}]BF_4$ (12). Complex 11 (100 mg, 0.141 mmol) was added to a solution of acetylacetonate (14.5 μ L, 0.141 mmol) and KOH (1.83 μ L, 0.224 M) in 10 mL of methanol. The mixture was stirred at room temperature for 24 h, and the solvent was removed under vacuum. The residue was treated with 15 mL of dichloromethane, and the resulting suspension was filtered over Celite. The yellow solution was concentrated under vacuum, and 5 mL of diethyl ether was added to precipitate a pale-yellow solid, which was washed with more diethyl ether (3×5 mL) and dried under vacuum. Yield: 50.3 mg (56%). X-ray quality crystals were grown by a slow diffusion of diethyl ether in a concentrated solution of the solid in dichloromethane at 4 °C. Anal. Calcd for $C_{24}H_{27}IrNO_2(BF_4)$: C, 45.01; H, 4.25; N, 2.19. Found: C, 45.13; H, 4.59; N, 2.05. HR-MS (electrospray): m/z calcd for $C_{24}H_{27}IrNO_2 [M]^+$ 554.1666; found 554.1699. IR (cm^{-1}): ν (BF_4) = 1049 (s). 1H NMR (300 MHz, CD_2Cl_2 , 298 K): δ 8.47 (ddd, 1H, $^3J_{H-H} = 6.1$; $^4J_{H-H} = 1.5$; $^5J_{H-H} = 0.8$, CH py), 8.10 (m, 1H, CH Ph), 8.03 (m, 1H, CH py), 7.87 (m, 3H, CH Ph), 7.49 (m, 2H, CH py), 5.55 (s, 1H, CH acac), 5.47 (m, 1H, =CH COD), 4.86 (m, 1H, =CH COD), 3.92 (m, 1H, =CH COD), 2.96 (m, 1H, =CH COD), 2.75 (m, 3H, CH_2 COD), 2.42 (s, 3H, acac), 2.30 (m, 3H, CH_2 COD), 1.80 (m, 2H, CH_2 COD), 1.66 (s, 3H, CH_3 acac). $^{13}C\{^1H\}$ NMR (75 MHz, CD_2Cl_2 , 298 K): δ 187.7 (C=O acac), 186.4 (C=O acac), 164.5 (C py), 150.5 (C Ph), 145.2 (CH py), 142.2 (C Ph), 141.5 (CH py), 134.4 (CH Ph) 132.9 (CH py), 126.8 (CH py) 125.4 (CH Ph) 124.5 (CH Ph) 121.4 (CH Ph), 101.9 (CH acac), 96.9, 92.5, 87.5, 85.6 (=CH COD), 34.8, 34.2, 29.6, 28.2 (CH_2 COD), 29.0, 27.7 (CH_2 acac).

Reaction of 12 with Acetylacetonate. Complex 12 (25 mg, 0.039 mmol) was added to a solution of KOH (12.9 mg, 0.195 mmol) and acetylacetonate (40.0 μ L, 0.390 mmol) in 5 mL of methanol. The mixture was stirred at room temperature for 24 h and dried under vacuum. The residue was treated with 15 mL of dichloromethane. The resulting yellow suspension was filtered over Celite. The yellow solution was concentrated almost to dryness. The subsequent addition of 5 mL of pentane led to 13, which was washed with 3×5 mL of pentane and dried under vacuum. Yield: 21.2 mg (83%).

Reaction of (2) with 2-(2-Bromophenyl)pyridine in 2-Ethoxyethanol. 2-(2-Bromophenyl)pyridine (210.3 μ L, 1.22 mmol) was added to 2 (200 mg, 0.298 mmol) in 8 mL of 2-ethoxyethanol. The resulting suspension was stirred at 135 °C overnight and subsequently was cooled to room temperature, dried under vacuum, and washed with methanol (3×5 mL). The obtained yellow solid was treated with 2×5 mL of dichloromethane to afford a new yellow suspension. The solid (21.4 mg) was separated by decantation and treated with acetylacetonate to yield 6 (<6%). The supernatant solution was filtered over Celite and concentrated under vacuum. The addition of pentane (5 mL) led to a white solid (113.7 mg) which was characterized as a 1.3:1 mixture of 9 (19%) and 13 (14%) by 1H NMR spectroscopy.

Preparation of $IrBr_2\{\kappa^2-C,N-[C_6H_4-py]\}\{\eta^4-C_8H_{12}\}$ (13). Silver tetrafluoroborate (303.7 mg, 1.56 mmol) was added to 2 (500 mg, 0.744 mmol) in 20 mL of acetone. The mixture was stirred for 1 h in the absence of light. The resulting suspension was filtered over Celite to obtain an orange solution, which was treated with 2-(2-bromophenyl)pyridine (525 μ L, 3.05 mmol). After 1 h, at room temperature, a white suspension was formed. The liquor was decanted and the white solid was washed with methanol (3×5 mL). Yield: 304.2 mg (37%). Anal. Calcd for $C_{19}H_{20}Br_2IrN$: C, 37.34; H, 3.28; N, 2.28. Found: C, 37.68; H, 3.25; N, 2.55. HR-MS (electrospray) m/z calcd. for $C_{19}H_{20}BrIrN [M - Br]^+$ 534.0373; found 534.0391. 1H NMR (300 MHz, CD_2Cl_2 , 298 K): δ 10.38 (d, 1H, $^3J_{H-H} = 6.1$, CH py), 8.01 (m, 1H, CH Ph), 7.97 (m, 1H, CH py), 7.83 (m, 2H, CH Ph + CH py), 7.48 (m, 1H, CH Ph), 7.31 (ddd, 1H, $^3J_{H-H} = 8.0$, 7.1; $^4J_{H-H} = 1.0$, CH Ph), 7.25 (ddd, 1H, $^3J_{H-H} = 7.6$, 6.2; $^4J_{H-H} = 1.6$, CH py), 5.80 (m, 1H, =CH COD), 5.17 (q, 1H, $^3J_{H-H} = 8.3$, =CH COD), 4.64 (td, 1H, $^3J_{H-H} = 8.6$, 4.4, =CH COD), 3.62 (tt, 1H,

$^3J_{\text{H-H}} = 13.8, 7.1, \text{CH}_2 \text{ COD}), 3.14 \text{ (m, 1H, =CH COD)}, 2.74 \text{ (td, 3H, } ^3J_{\text{H-H}} = 13.5, 8.5, \text{CH}_2 \text{ COD)}, 2.14 \text{ (m, 2H, CH}_2 \text{ COD)} \text{ and } 1.65 \text{ (m, 2H, CH}_2 \text{ COD)}. ^{13}\text{C}\{^1\text{H}\} \text{ NMR (75 MHz, CD}_2\text{Cl}_2, 298 \text{ K): } \delta \text{ 171.1 (C, py), 162.3 (C, Ph), 152.3 (CH, py), 143.9 (C, Ph), 139.2 (CH, Ph), 134.9 (CH, Ph), 132.5 (CH, Ph), 125.3 (CH, py), 124.9 (CH, Ph) 123.4 (CH, py), 120.4 (CH, py), 99.0, 90.8, 87.5, 85.2 (=CH, COD), 35.5, 33.7, 30.0, 28.2 (CH}_2 \text{ COD)}.$

■ ASSOCIATED CONTENT

Supporting Information

The Supporting Information is available free of charge on the ACS Publications website at DOI: 10.1021/acs.organomet.8b00500.

Instrumental methods; ORTEP diagrams of complexes **11** and **12**; structural analysis of complexes **5**, **6**, **9**, **10**, **11**, and **12**; MALDI-TOF spectra of complexes **3** and **5**; ^1H NMR for complex **5**; and ^1H NMR and $^{13}\text{C}\{^1\text{H}\}$ ATP NMR of complexes **6**, **8**, **9**, **10**, **11**, **12**, and **13** (PDF)

Accession Codes

CCDC 1854811–1854816 contain the supplementary crystallographic data for this paper. These data can be obtained free of charge via www.ccdc.cam.ac.uk/data_request/cif, or by emailing data_request@ccdc.cam.ac.uk, or by contacting The Cambridge Crystallographic Data Centre, 12 Union Road, Cambridge CB2 1EZ, UK; fax: +44 1223 336033.

■ AUTHOR INFORMATION

Corresponding Author

*E-mail: maester@unizar.es.

ORCID

Miguel A. Esteruelas: 0000-0002-4829-7590

Enrique Oñate: 0000-0003-2094-719X

Notes

The authors declare no competing financial interest.

■ ACKNOWLEDGMENTS

Financial support from the MINECO of Spain (Projects CTQ2017-82935-P and Red de Excelencia Consolider CTQ2016-81797-REDC), the Diputación General de Aragón (E06_17R), FEDER, and the European Social Fund is acknowledged.

■ REFERENCES

- (1) (a) Littke, A. F.; Fu, G. C. Palladium-catalyzed coupling reactions of aryl chlorides. *Angew. Chem., Int. Ed.* **2002**, *41*, 4176–4211. (b) Johansson Seechurn, C. C. C.; Kitching, M. O.; Colacot, T. J.; Snieckus, V. Palladium-catalyzed cross-coupling: A historical contextual perspective to the 2010 nobel prize. *Angew. Chem., Int. Ed.* **2012**, *51*, 5062–5085. (c) Han, F. S. Transition-metal-catalyzed Suzuki-Miyaura cross-coupling reactions: A remarkable advance from palladium to nickel catalysts. *Chem. Soc. Rev.* **2013**, *42*, 5270–5298. (d) Ruiz-Castillo, P.; Buchwald, S. L. Applications of Palladium-Catalyzed C–N Cross-Coupling Reactions. *Chem. Rev.* **2016**, *116*, 12564–12649.
- (2) (a) Cavallo, G.; Metrangolo, P.; Milani, R.; Pilati, T.; Priimagi, A.; Resnati, G.; Terraneo, G. The halogen bond. *Chem. Rev.* **2016**, *116*, 2478–2601. (b) Eisenstein, O.; Milani, J.; Perutz, R. N. Selectivity of C–H Activation and Competition between C–H and C–F Bond Activation at Fluorocarbons. *Chem. Rev.* **2017**, *117*, 8710–8753.
- (3) Hartwig, J. F. Evolution of C–H Bond Functionalization from Methane to Methodology. *J. Am. Chem. Soc.* **2016**, *138*, 2–24.

- (4) (a) Balcells, D.; Clot, E.; Eisenstein, O. C–H Bond Activation in Transition Metal Species from a Computational Perspective. *Chem. Rev.* **2010**, *110*, 749–823. (b) Esteruelas, M. A.; Oliván, M.; Vélez, A. POP–Rhodium-Promoted C–H and B–H Bond Activation and C–B Bond Formation. *Organometallics* **2015**, *34*, 1911–1924. (c) Esteruelas, M. A.; López, A. M.; Oliván, M. Polyhydrides of Platinum Group Metals: Nonclassical Interactions and σ -Bond Activation Reactions. *Chem. Rev.* **2016**, *116*, 8770–8847.

(5) Corbet, J.-P.; Mignani, G. Selected Patented Cross-Coupling Reaction Technologies. *Chem. Rev.* **2006**, *106*, 2651–2710.

(6) Alonso, F.; Beletskaya, I. P.; Yus, M. Metal-mediated reductive hydrodehalogenation of organic halides. *Chem. Rev.* **2002**, *102*, 4009–4091.

(7) Gildner, P. G.; Colacot, T. J. Reactions of the 21st Century: Two Decades of Innovative Catalyst Design for Palladium-Catalyzed Cross-Couplings. *Organometallics* **2015**, *34*, 5497–5508.

- (8) (a) Butts, M. D.; Scott, B. L.; Kubas, G. J. Syntheses and structures of alkyl and aryl halide complexes of the type $[(\text{P}i\text{Pr}_3)_2\text{PtH}(\eta^1\text{-XR})]\text{BAR}_f$ and analogues with Et_2O , THF, and H_2 ligands. Halide-to-metal π bonding in halocarbon complexes. *J. Am. Chem. Soc.* **1996**, *118*, 11831–11843. (b) Lucassen, A. C. B.; Shimon, L. J. W.; Van Der Boom, M. E. Formation of fluorinated platinum-stilbazole complexes: Aryl-halide oxidative addition vs η^2 -coordination of a carbon-carbon double bond. *Organometallics* **2006**, *25*, 3308–3310. (c) Naya, L.; Vázquez-García, D.; López-Torres, M.; Fernández, A.; Vila, J. M.; Gómez-Blanco, N.; Fernández, J. J. Activation of C–H and C–Br bonds in cyclopalladation reactions of Schiff base ligands: Influence of the benzylidene ring substituents. *J. Organomet. Chem.* **2008**, *693*, 685–700. (d) Naya, L.; Vázquez-García, D.; López-Torres, M.; Fernández, A.; Rodríguez, A.; Gómez-Blanco, N.; Vila, J. M.; Fernández, J. J. Mononuclear and tetranuclear palladacycles with terdentate $[\text{C},\text{N},\text{N}]$ and $[\text{C},\text{N},\text{O}]$ Schiff base ligands. C–H versus C–Br activation reactions. *Inorg. Chim. Acta* **2011**, *370*, 89–97. (e) Cariou, R.; Graham, T. W.; Dahcheh, F.; Stephan, D. W. Oxidative addition of aryl halides: Routes to mono- and dimetallic nickel amino-bisphosphinimine complexes. *Dalton Trans.* **2011**, *40*, 5419–5422. (f) Li, J.; Wang, C.; Li, X.; Sun, H. C–Cl bond activation of ortho-chlorinated benzamides by nickel and cobalt compounds supported with phosphine ligands. *Dalton Trans.* **2012**, *41*, 8715–8722. (g) Anderson, C. M.; Oh, N.; Balema, T. A.; Mastrocinque, F.; Mastrocinque, C.; Santos, D.; Greenberg, M. W.; Tanski, J. M. Regioselective C–H/C–X activation of naphthyl-derived ligands to form six-membered palladacycles. *Tetrahedron Lett.* **2016**, *57*, 4574–4577.

- (9) (a) Bedford, R. B.; Limmert, M. E. Catalytic Intermolecular Ortho-Arylation of Phenols. *J. Org. Chem.* **2003**, *68*, 8669–8682. (b) Lewis, J. C.; Wiedemann, S. H.; Bergman, R. G.; Ellman, J. A. Arylation of Heterocycles via Rhodium-Catalyzed C–H Bond Functionalization. *Org. Lett.* **2004**, *6*, 35–38. (c) Ueura, K.; Satoh, T.; Miura, M. Rhodium-Catalyzed Arylation Using Arylboron Compounds: Efficient Coupling with Aryl Halides and Unexpected Multiple Arylation of Benzonitrile. *Org. Lett.* **2005**, *7*, 2229–2231. (d) Takahashi, H.; Inagaki, S.; Nishihara, Y.; Shibata, T.; Takagi, K. Novel Rh Catalysis in Cross-Coupling between Alkyl Halides and Arylzinc Compounds Possessing *ortho*-COX (X = OR, NMe₂, or Ph) Groups. *Org. Lett.* **2006**, *8*, 3037–3040. (e) Kim, M.; Chang, S. Rhodium(NHC)-Catalyzed Amination of Aryl Bromides. *Org. Lett.* **2010**, *12*, 1640–1643. (f) Jiang, Q.; Guo, T.; Wang, Q.; Wu, P.; Yu, Z. Rhodium(I)-Catalyzed Arylation of β -Chloro Ketones and Related Derivatives through Domino Dehydrochlorination/Conjugate Addition. *Adv. Synth. Catal.* **2013**, *355*, 1874–1880.

- (10) (a) Esteruelas, M. A.; Herrero, J.; López, F. M.; Martín, M.; Oro, L. A. Dehalogenation of Polychloroarenes with HSiEt_3 Catalyzed by an Homogeneous Rhodium–Triphenylphosphine System. *Organometallics* **1999**, *18*, 1110–1112. (b) Díaz, J.; Esteruelas, M. A.; Herrero, J.; Moralejo, L.; Oliván, M. Simultaneous Dehalogenation of Polychloroarenes and Chlorination of HSiEt_3 Catalyzed by Complexes of the Groups 8 and 9. *J. Catal.* **2000**, *195*, 187–192. (c) Fujita, K.; Owaki, M.; Yamaguchi, R. Chemoselective transfer hydro-

dechlorination of aryl chlorides catalyzed by Cp*Rh complexes. *Chem. Commun.* **2002**, 2964–2965. (d) Esteruelas, M. A.; Herrero, J.; Oliván, M. Dehalogenation of Hexachlorocyclohexanes and Simultaneous Chlorination of Triethylsilane Catalyzed by Rhodium and Ruthenium Complexes. *Organometallics* **2004**, *23*, 3891–3897. (e) Buil, M. L.; Esteruelas, M. A.; Niembro, S.; Oliván, M.; Orzechowski, L.; Pelayo, C.; Vallribera, A. Dehalogenation and Hydrogenation of Aromatic Compounds Catalyzed by Nanoparticles Generated from Rhodium Bis(imino)pyridine Complexes. *Organometallics* **2010**, *29*, 4375–4383.

(11) (a) Willems, S. T. H.; Budzelaar, P. H. M.; Moonen, N. N. P.; de Gelder, R.; Smits, J. M. M.; Gal, A. W. Coordination and Oxidative Addition at a Low-Coordinate Rhodium(I) β -Diimine Centre. *Chem. - Eur. J.* **2002**, *8*, 1310–1320. (b) Grushin, V. V.; Marshall, W. J. The Fluoro Analogue of Wilkinson's Catalyst and Unexpected Ph-Cl Activation. *J. Am. Chem. Soc.* **2004**, *126*, 3068–3069. (c) Macgregor, S. A.; Roe, D. C.; Marshall, W. J.; Bloch, K. M.; Bakhtmutov, V. I.; Grushin, V. V. The F/Ph rearrangement reaction of $[(\text{Ph}_3\text{P})_3\text{RhF}]$, the fluoride congener of Wilkinson's catalyst. *J. Am. Chem. Soc.* **2005**, *127*, 15304–15321. (d) Gatard, S.; Çelenligil-Çetin, R.; Guo, C.; Foxman, B. M.; Ozerov, O. V. Carbon-halide oxidative addition and carbon-carbon reductive elimination at a (PNP)Rh center. *J. Am. Chem. Soc.* **2006**, *128*, 2808–2809. (e) Gatard, S.; Guo, C.; Foxman, B. M.; Ozerov, O. V. Thioether, dinitrogen, and olefin complexes of (PNP)Rh: Kinetics and thermodynamics of exchange and oxidative addition reactions. *Organometallics* **2007**, *26*, 6066–6075. (f) Douglas, T. M.; Chaplin, A. B.; Weller, A. S. Dihydrogen loss from a 14-electron rhodium(III) bis-phosphine dihydride to give a rhodium(I) complex that undergoes oxidative addition with aryl chlorides. *Organometallics* **2008**, *27*, 2918–2921. (g) Ito, J. I.; Miyakawa, T.; Nishiyama, H. Amine-assisted C-Cl bond activation of aryl chlorides by a (phebox)Rh-chloro complex. *Organometallics* **2008**, *27*, 3312–3315. (h) Puri, M.; Gatard, S.; Smith, D. A.; Ozerov, O. V. Competition studies of oxidative addition of aryl halides to the (PNP) Rh fragment. *Organometallics* **2011**, *30*, 2472–2482. (i) Pike, S. D.; Weller, A. S. C-Cl activation of the weakly coordinating anion $[\text{B}(3,5\text{-Cl}_2\text{C}_6\text{H}_3)_4]^-$ at a Rh(I) centre in solution and the solid-state. *Dalton Trans.* **2013**, *42*, 12832–12835. (j) Qian, Y. Y.; Lee, M. H.; Yang, W.; Chan, K. S. Aryl carbon-chlorine (Ar-Cl) and aryl carbon-fluorine (Ar-F) bond cleavages by rhodium porphyrins. *J. Organomet. Chem.* **2015**, *791*, 82–89. (k) Curto, S. G.; Esteruelas, M. A.; Oliván, M.; Oñate, E.; Vélez, A. Selective C-Cl bond oxidative addition of chloroarenes to a POP-rhodium complex. *Organometallics* **2017**, *36*, 114–128.

(12) Wu, H.; Hall, M. B. Kinetic C-H oxidative addition vs thermodynamic C-X oxidative addition of chlorobenzene by a neutral Rh(I) system. A density functional theory study. *J. Phys. Chem. A* **2009**, *113*, 11706–11712.

(13) Ben-Ari, E.; Cohen, R.; Gandelman, M.; Shimon, L. J. W.; Martin, J. M. L.; Milstein, D. *ortho* C-H Activation of Haloarenes and Anisole by an Electron-Rich Iridium(I) Complex: Mechanism and Origin of Regio- and Chemoselectivity. An Experimental and Theoretical Study. *Organometallics* **2006**, *25*, 3190–3210.

(14) Fan, L.; Parkin, S.; Ozerov, O. V. Halobenzenes and Ir(I): Kinetic C-H oxidative addition and thermodynamic C-Hal oxidative addition. *J. Am. Chem. Soc.* **2005**, *127*, 16772–16773.

(15) Wu, H.; Hall, M. B. Carbon-hydrogen vs. Carbon-halogen oxidative addition of chlorobenzene by a neutral iridium complex explored by DFT. *Dalton Trans.* **2009**, 5933–5942.

(16) (a) Ros, A.; Fernández, R.; Lassaletta, J. M. Functional group directed C-H borylation. *Chem. Soc. Rev.* **2014**, *43*, 3229–3243. (b) Yadav, M. R.; Rit, R. K.; Shankar, M.; Sahoo, A. K. Reusable and Removable Directing Groups for C(sp²)-H Bond Functionalization of Arenes. *Asian J. Org. Chem.* **2015**, *4*, 846–864.

(17) Albrecht, M. Cyclometalation Using d-Block Transition Metals: Fundamental Aspects and Recent Trends. *Chem. Rev.* **2010**, *110*, 576–623.

(18) Matsubara, T.; Koga, N.; Musaev, D. G.; Morokuma, K. Density Functional Study on Highly Ortho-Selective Addition of an

Aromatic CH Bond to Olefins Catalyzed by a Ru(H)₂(CO)(PR₃)₃ Complex. *Organometallics* **2000**, *19*, 2318–2329.

(19) (a) Zhang, X.; Kanzelberger, M.; Emge, T. J.; Goldman, A. S. Selective Addition to Iridium of Aryl C-H Bonds Ortho to Coordinating Groups. Not Chelation-Assisted. *J. Am. Chem. Soc.* **2004**, *126*, 13192–13193. (b) Alós, J.; Esteruelas, M. A.; Oliván, M.; Oñate, E.; Puylaert, P. C-H Bond Activation Reactions in Ketones and Aldehydes Promoted by POP-Pincer Osmium and Ruthenium Complexes. *Organometallics* **2015**, *34*, 4908–4921.

(20) (a) Esteruelas, M. A.; Oro, L. A. Iridium and rhodium complexes with tetrafluorobenzobarrelene diolefins. *Coord. Chem. Rev.* **1999**, *193*–195, 557–618. (b) Peruzzini, M.; Bianchini, C.; Gonsalvi, L. In *Comprehensive Organometallic Chemistry III*; Crabtree, R. H., Mingos, D. M. P., Eds.; Elsevier: Amsterdam, 2007; Chapter 7.04, pp 267–425.

(21) Polborn, K.; Severin, K. Heterobimetallic and mixed-valence chloro-bridged complexes with orthometalated rhodium(III) and iridium(III) fragments. *Eur. J. Inorg. Chem.* **1998**, *1998*, 1187–1192.

(22) (a) Bennett, M. A.; Patmore, D. J. Four- and five-coordinate complexes of rhodium and iridium containing trifluorophosphine. *Inorg. Chem.* **1971**, *10*, 2387–2395. (b) Diversi, P.; Ingrosso, G.; Immirzi, A.; Porzio, W.; Zocchi, M. The reaction of allene with β -diketonatoiridium(I) complexes: synthesis, properties and crystal structures of bis(η^3 -allylic) complexes of iridium(III) and of iridocyclopentane derivatives. *J. Organomet. Chem.* **1977**, *125*, 253–271.

(23) (a) Böttcher, H.-C.; Graf, M.; Sünkel, K.; Mayer, P.; Krüger, H. $[\text{Ir}(\text{acac})(\eta^2\text{-C}_8\text{H}_{14})_2]$: A precursor in the synthesis of cyclometalated iridium(III) complexes. *Inorg. Chim. Acta* **2011**, *365*, 103–107.

(b) Baranoff, E.; Curchod, B. F. E.; Frey, J.; Scopelliti, R.; Kessler, F.; Tavernelli, I.; Rothlisberger, U.; Grätzel, M.; Nazeeruddin, M. K. Acid-induced degradation of phosphorescent dopants for OLEDs and its application to the synthesis of tris-heteroleptic iridium(III) bis-cyclometalated complexes. *Inorg. Chem.* **2012**, *51*, 215–224.

(24) (a) Johnson, C. E.; Eisenberg, R. Stereoselective oxidative addition of silanes and hydrogen halides to the iridium(I) cis phosphine complexes $\text{IrX}(\text{CO})(\text{dppe})$ (X = Br, CN; dppe = 1,2-bis(diphenylphosphino)ethane). *J. Am. Chem. Soc.* **1985**, *107*, 6531–6540. (b) Esteruelas, M. A.; Lahoz, F. J.; Oliván, M.; Oñate, E.; Oro, L. A. Oxidative Addition of HSnR_3 (R = Ph, ⁿBu) to the Square-Planar Iridium(I) Compounds $\text{Ir}(\text{XR})(\text{TfB})(\text{PCy}_3)$ (XR = OMe, OEt, OⁿPr, OPh, SⁿPr) and $\text{Ir}(\text{C}_2\text{Ph})\text{L}_2(\text{PCy}_3)$ (L₂ = TfB, 2CO). *Organometallics* **1995**, *14*, 3486–3496. (c) Esteruelas, M. A.; Oliván, M.; Oro, L. A. Reactions of the Square-Planar Compounds $\text{Ir}(\text{C}_2\text{Ph})\text{L}_2(\text{PCy}_3)$ (L₂ = 2 CO, TfB) with HSiR_3 (R = Et, Ph) and $\text{H}_{x+1}\text{SiPh}_{3-x}$ (x = 1, 2): Stoichiometric and Catalytic Formation of Si-C Bonds. *Organometallics* **1996**, *15*, 814–822. (d) Esteruelas, M. A.; Oliván, M.; Velez, A. Xantphos-Type Complexes of Group 9: Rhodium versus Iridium. *Inorg. Chem.* **2013**, *52*, 5339–5349. (e) Alabau, R. G.; Esteruelas, M. A.; Oliván, M.; Oñate, E.; Palacios, A. U.; Tsai, J.-Y.; Xia, C. Osmium(II) Complexes Containing a Dianionic CCCC-Donor Tetradentate Ligand. *Organometallics* **2016**, *35*, 3981–3995.

(25) Churchill, M. R.; Bezman, S. A. X-ray crystallographic studies on fluxional pentacoordinate transition metal complexes. III. (Cycloocta-1,5-diene)[bis(1,3-diphenylphosphino)propane]methyliridium(I). *Inorg. Chem.* **1973**, *12*, 531–536.

(26) (a) Fernandez, M. J.; Esteruelas, M. A.; Oro, L. A.; Aprea, M. C.; Foces-Foces, C.; Cano, F. H. Preparation, properties, and reactivity of dihydridosilyl(η^4 -cycloocta-1,5-diene)iridium(III) complexes. X-ray crystal structures of the dihydrido silyl complex $\text{IrH}_2(\text{SiEt}_3)(\eta^4\text{-C}_8\text{H}_{12})(\text{AsPh}_3)$ and the cyclooctenyl derivative $\text{Ir}(1\text{-}\sigma,4,5\text{-}\eta^2\text{-C}_8\text{H}_{13})(\text{CO})_2(\text{AsPh}_3)$. *Organometallics* **1987**, *6*, 1751–1756. (b) Bianchini, C.; Farnetti, E.; Graziani, M.; Nardin, G.; Vacca, A.; Zanobini, F. Electron-rich iridium complexes with mixed-donor polydentate ligands. Chemoselective catalysts in hydrogen-transfer reduction of α,β -unsaturated ketones. *J. Am. Chem. Soc.* **1990**, *112*, 9190–9197. (c) Nguyen, D. H.; Greger, I.; Pérez-Torrente, J. J.; Jiménez, M. V.; Modrego, F. J.; Lahoz, F. J.; Oro, L. A. ONO

Dianionic Pincer-Type Ligand Precursors for the Synthesis of σ,π -Cyclooctenyl Iridium(III) Complexes: Formation Mechanism and Coordination Chemistry. *Organometallics* **2013**, *32*, 6903–6917. (d) Nguyen, D. H.; Pérez-Torrente, J. J.; Jiménez, M. V.; Modrego, F. J.; Gómez-Bautista, D.; Lahoz, F. J.; Oro, L. A. Unsaturated Iridium(III) Complexes Supported by a Quinolato–Carboxylato ONO Pincer-Type Ligand: Synthesis, Reactivity, and Catalytic C–H Functionalization. *Organometallics* **2013**, *32*, 6918–6930. (e) Padilla-Martínez, I. I.; Cervantes-Vásquez, M.; Leyva-Ramírez, M. A.; Paz-Sandoval, M. A. Iridaoxacyclohexadiene-Bridged Mixed-Valence Iridium Cyclooctadiene Complex: Oxidative Addition and Hydrogen-Transfer to Coordinated Cyclooctadiene. *Organometallics* **2014**, *33*, 6305–6318.

(27) (a) Esteruelas, M. A.; Oliván, M.; Oro, L. A.; Schulz, M.; Sola, E.; Werner, H. Synthesis, molecular structure and reactivity of the octahedral iridium(III) compound $[\text{IrH}(\eta^1, \eta^3\text{-C}_8\text{H}_{12})(\text{dppm})]$ [dppm = bis(diphenylphosphino)methane]. *Organometallics* **1992**, *11*, 3659–3664. (b) Serrano, O.; Nicasio-Collazo, J.; Morales, G.; Alvarado-Monzón, J. C.; Torres-Huerta, A.; Höpfl, H.; López, J. A.; Esqueda, A. C. Synthesis and Characterization of $[\text{Ir}(\text{Acac}^{\text{BiMs}})(\text{COD})]$ and $[\text{cis-Ir}(\text{Acac}^{\text{BiMs}})_2(\text{COE-OH})]$. *Organometallics* **2014**, *33*, 2561–2564.

(28) Eisenstein, O.; Hoffmann, R. Activation of a coordinated olefin toward nucleophilic attack. *J. Am. Chem. Soc.* **1980**, *102*, 6148–6149.

(29) van der Ent, A.; Onderdelinden, A. L.; Schunn, R. A. Chlorobis(cyclooctene)rhodium(I) and -iridium(I) complexes. *Inorg. Synth.* **2007**, *28*, 90–92.